

## Layer-by-layer deposition of $\text{CoFe}_2\text{O}_4$ nanocrystals onto unbleached pulp fibres for producing magnetic paper

Chin Hua Chia<sup>\*1</sup>, Sarani Zakaria<sup>1</sup>, Seng Chau Goh<sup>1</sup>, Chi Hoong Chan<sup>1</sup>

<sup>1</sup>School of Applied Physics Faculty of Science and Technology, Universiti Kebangsaan Malaysia, 43600 Bangi Selangor, Malaysia

\*Corresponding author's phone: +603-8921 5473

E-mail: chiachinhua@yahoo.com / chia@ukm.my

Date Received 5<sup>th</sup> September 2013

Date Revised 4<sup>th</sup> December 2013

Date Accepted 11<sup>th</sup> December 2013

### ABSTRACT

Magnetic fibres were prepared by layer-by-layer (LBL) deposition of cobalt ferrite ( $\text{CoFe}_2\text{O}_4$ ) nanocrystals onto unbleached kenaf pulp fibres. Polyacrylamide (PAM) was used to change the negative charge of the pulp fibre to positive so that the negatively charged  $\text{CoFe}_2\text{O}_4$  nanocrystals could be readily deposited onto the surface of the fibres. The deposition of  $\text{CoFe}_2\text{O}_4$  nanocrystals onto fibre increased linearly to 115 mg/g of fibre deposited with 40 wt%  $\text{CoFe}_2\text{O}_4$  nanocrystals solution and started to fluctuate after the addition of 40 wt% which could probably be due to no more available sites on the fibre for further deposition of the  $\text{CoFe}_2\text{O}_4$  nanocrystals. Magnetic paper was formed using layer-by-layer deposition on fibres by adding 40 wt%  $\text{CoFe}_2\text{O}_4$  nanocrystals for each layer. The degree of magnetic loading and magnetic properties could be adjusted by varying the number of deposition layers. LbL deposition method produced magnetic fibres with better retention than that of in situ synthesis method.

Keywords: Cobalt ferrite; magnetic fibres; magnetic nanoparticles; polyacrylamide

## 1.0 INTRODUCTION

Lignocellulosic fibres possess magnetic properties offer opportunities to the exploration of new concepts in papermaking which will revolutionize the application of papers, including security paper, high density magnetic recording medium, electromagnetic shielding, reprographic printing and magnetic filtering [1].

To the best of our knowledge, there are three methods reported previously in the preparation of magnetic paper, i.e., lumen loading [2], *in situ* synthesis [3] and nano-coating [4]. These studies have utilized magnetite ( $\text{Fe}_3\text{O}_4$ ) particles as magnetic pigment. However, to produce magnetic paper for magnetic recording purposes, the coercivity of the magnetic pigment has to be high enough to achieve high recording density and stable storage [5,6].

For the past decade, layer-by-layer (LbL) assembly approach in synthesizing new materials have been gaining traction especially in the fields of drug delivery [7]. In a study by Lu [8], paper containing titanium dioxide nanoparticles had been produced using LbL assembly. In this method, pulp fibres were alternately soaked into polyelectrolyte solution and titanium dioxide filler suspension to create multilayer of filler. This method offers a new concept in the preparation of filler loaded paper, which will provide better paper strength as compared to conventional methods. LbL assembly is based on adsorption of oppositely charged polyelectrolytes and fillers from their solutions in alternate steps. The interaction involves is assumed to be electrostatic.

In papermaking process, there are various types of polymers which have been used as retention aid to provide a strong adhesion of filler onto fibre mat, such as polyacrylamide [9-11], polyethylenimine [12], polyethylene oxide [13], alum [14], cationic starch [15], polydimethyldiallylammonium chloride and 3–6 ionene [16]. In this study, cationic PAM has been used to reverse the negative charge of the unbleached pulp fibres to allow the deposition of  $\text{CoFe}_2\text{O}_4$  nanocrystals. The cobalt ferrite ( $\text{CoFe}_2\text{O}_4$ ) nanocrystals used in this study were

synthesized using co-precipitation technique [5]. CoFe<sub>2</sub>O<sub>4</sub> possesses stronger coercivity as compared to Fe<sub>3</sub>O<sub>4</sub>[17], which is more suitable for magnetic recording purposes. The main focus of this study is to investigate the optimum deposition degree of CoFe<sub>2</sub>O<sub>4</sub> nanocrystals onto the unbleached pulp fibre for creation of a uniform deposition layer. LbL deposition was performed on the uniform deposited layer, so as to obtain a higher magnetic coercivity. In our previous study [5], it was reported that a tremendous loss of paper strength, as much as 86.3% with 21.0 wt% degree of loading due to the presence of large amount of magnetic particles on the fibre surface. Therefore this study is crucial for producing high strength magnetic paper with a high degree of loading.

## **2.0 MATERIALS AND METHODS**

### **2.1 Materials**

Unbleached kenaf pulp was prepared by cooking the kenaf wood chips with 14 % active alkali, 25 % sulfidity, at 170 °C for 3 h (including 90 min to raise the temperature to maximum). The pulp yield was ~40.4 % (Kappa number ~50). Ferric chloride (FeCl<sub>3</sub>), cobalt chloride hexahydrate (CoCl<sub>2</sub> • 6H<sub>2</sub>O), hydrochloric acid (HCl) and sodium hydroxide (NaOH) were purchased from Merck Co. PAM with mass-average molecular weight of 1,500 was acquired from Aldrich Chemical Co. All chemicals were used without further purification.

### **2.2 Synthesis of CoFe<sub>2</sub>O<sub>4</sub> Nanocrystals**

CoCl<sub>2</sub> • 6H<sub>2</sub>O and FeCl<sub>3</sub> at a 1:2 molar ratio were dissolved into a round bottom flask containing 200 mL of distilled water at 100 °C. While vigorously stirred by mechanical stirrer, NaOH was added into the mixture to initiate the formation of ferrite structure. The temperature was maintained constant throughout the reaction time of 60 min to allow the

crystal growth. The resulting black precipitate in the flask was separated by placing onto a permanent magnet to accelerate the settling. The clear salt solution was decanted. The precipitate was washed through several cycles with distilled water and kept in refrigerator for characterizations and deposition studies. The obtained  $\text{CoFe}_2\text{O}_4$  crystals were characterized by X-ray diffractometer (XRD), transmission electron microscope (TEM), and vibrating sample magnetometer (VSM).

### 2.3 Surface Charge Measurement – Unbleached Kenaf Pulp Fibre and $\text{CoFe}_2\text{O}_4$ Nanocrystals

The surface charge of the pulp fibres and  $\text{CoFe}_2\text{O}_4$  nanocrystals was measured using ZetaSizer (Malvern) at 25 °C. The pH of the suspension was adjusted using HCl (0.1 M) and NaOH (0.1 M).

### 2.4 Deposition of $\text{CoFe}_2\text{O}_4$ Nanocrystals onto Fibres

Distilled water at pH 8.5 was prepared using HCl and NaOH and it was used throughout the deposition study. Unbleached kenaf pulp (500 mg oven dry) was dispersed into 490 mL distilled water under vigorous stirring at 250 rpm. Ten milliliters of PAM (0.2 wt% to pulp fibres) was added into the pulp suspension and left to stir for 15 min. The pulp fibres were then rinsed several times with distilled water to remove the excess PAM and re-dispersed into 490 mL distilled water. Ten milliliters  $\text{CoFe}_2\text{O}_4$  suspension (5 wt% to pulp fibre) was added into the pulp suspension and left to stir for 15 min. The sample of the supernatant (~10 mL) was withdrawn using a pipette, while a small amount of pulp fibres was collected for characterizations. 1 mL of 1.0 M HCl was added into the supernatant sample to dissolve the  $\text{CoFe}_2\text{O}_4$  nanocrystals and followed by the measurements of the concentration of Co using an Inductive Coupled Plasma Mass Spectrometer (ICP-MS),

representing the undeposited  $\text{CoFe}_2\text{O}_4$  nanocrystals. After that, 10 mL of  $\text{CoFe}_2\text{O}_4$  (5 wt% to pulp fibre) was again added into the pulp suspension with continuous stirring for another 15 min before the pulp supernatant sample was withdrawn again. The total volume of the pulp suspension was maintained at 500 mL throughout the experiment. This procedure was repeated until 100 wt% of  $\text{CoFe}_2\text{O}_4$  nanocrystals was added.

## 2.5 Layer-by-Layer Deposition

Once the optimum concentration of  $\text{CoFe}_2\text{O}_4$  nanocrystals single layer deposition is obtained, LbL deposition is conducted. The fibres were dispersed in distilled water; PAM solution of (0.2 wt% to pulp fibres) was added into the pulp suspension and left to stir for 15 min, then rinsed several times with distilled water to remove the excess PAM and re-dispersed into distilled water.  $\text{CoFe}_2\text{O}_4$  nanocrystals of optimum deposition concentration were added into the pulp suspension and left to stir for 15 min. Three samples of different deposition layers, i.e., 1-layer, 3-layers and 5-layers, were produced.

## 2.6 Papermaking: Preparations and Testings

Magnetic papers were prepared and tested in accordance to the standards of the Technical Association of the Pulp and Paper Industry (T 425 om-96, T 452 om-98, T 494 om-96, T 220 sp-96) using the magnetic fibres.

## 2.7 Characterization of Magnetic Fibres

The magnetic properties of the magnetic fibres were measured using a vibrating sample magnetometer (VSM, Lakeshore 736) with a maximum field of 10 kOe at room temperature. The deposition of the  $\text{CoFe}_2\text{O}_4$  nanocrystals on the pulpfibres before and after

the papermaking process was examined using a scanning electron microscope (SEM, Leo-150 VP).

### 3.0 RESULTS AND DISCUSSION

#### 3.1 Characterization of the CoFe<sub>2</sub>O<sub>4</sub> Nanocrystals

The XRD pattern shown in Figure 1(a) confirms the formation of ferrite structure of the CoFe<sub>2</sub>O<sub>4</sub> nanocrystals. The diffraction peaks are corresponding to the cubic inverse spinel type lattice of CoFe<sub>2</sub>O<sub>4</sub> (JCPDS Card No. 22-1086). The strong and sharp diffraction peaks indicate the high crystallinity of the nanocrystals. The lattice parameter estimated from the strongest diffraction peak of (311) is  $\sim 8.380$  Å, which is consistent with the bulk value 8.377 Å of CoFe<sub>2</sub>O<sub>4</sub>. Figure 1 (b) shows the TEM image of the produced CoFe<sub>2</sub>O<sub>4</sub> nanocrystals. It can be clearly seen that the nanocrystals possess well-defined spherical shape at an average crystal size  $\sim 17.0 \pm 1.4$  nm. The *M-H* loop of the CoFe<sub>2</sub>O<sub>4</sub> nanocrystals is shown in Figure 1(c). The saturation magnetization and coercivity of the CoFe<sub>2</sub>O<sub>4</sub> nanocrystals are 36.4 emu/g and 250 Oe, respectively, suggesting that it is suitable to be used as magnetic pigment for magnetic recording application, as compared to Fe<sub>3</sub>O<sub>4</sub> nanocrystals which possesses superparamagnetic properties [5].

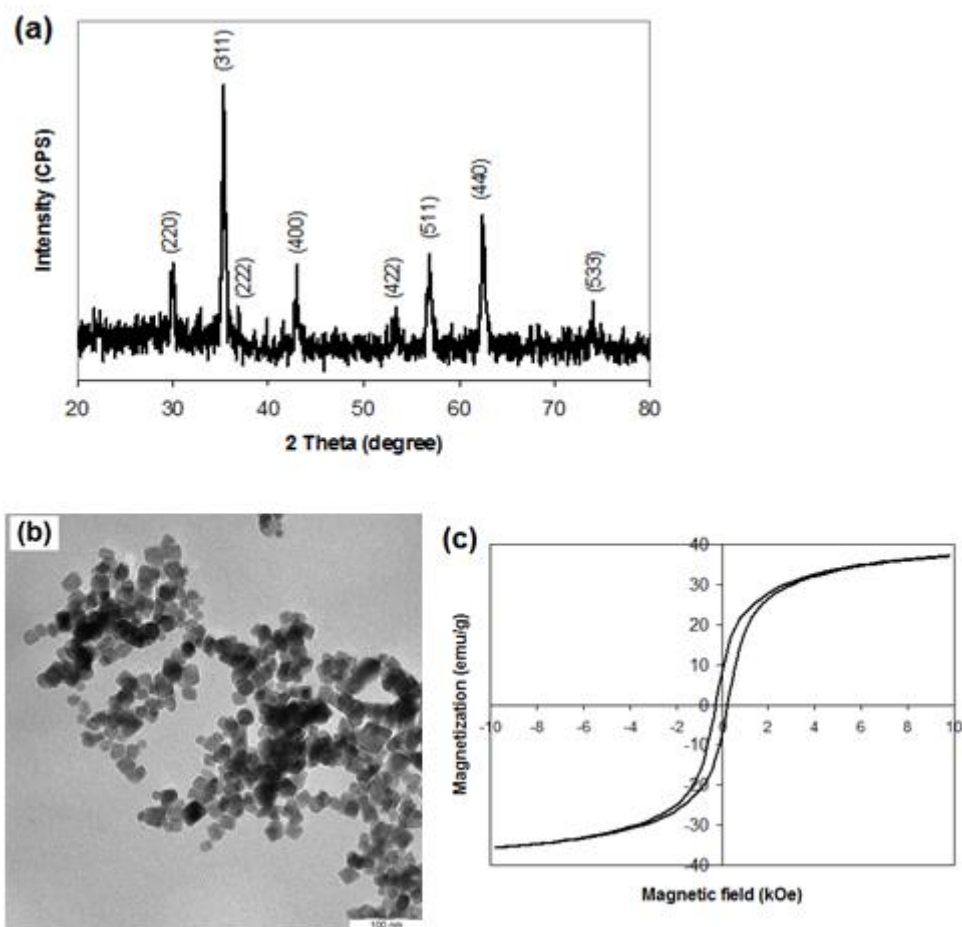


Figure 1: Characterization results of the  $\text{CoFe}_2\text{O}_4$  nanocrystals produced via co-precipitation method: (a) XRD pattern, (b) TEM image, and (c) M-H loop

### 3.2 Surface Charges of the Unbleached Pulp Fibres and $\text{CoFe}_2\text{O}_4$ Nanocrystals

Figure 2 presents the zeta potential results for untreated and PAM treated kenaf pulp fibres and  $\text{CoFe}_2\text{O}_4$  nanocrystals at different pH. These results represent the surface charge of the samples. It can be seen that the untreated kenaf pulp fibres are solely negative charge at the pH ranging from 3 to 11. This is associated with the carboxylic and phenolic groups in the unbleached kenaf pulp fibres. It is also noted that the fibre charge is increased with pH which is attributed to the ionization of the carboxylic and phenolic groups of the lignocellulosic fibres at high pH [18]. After the PAM treatment, the fibre charge is converted into positive at the entire pH ranging from 3 to 11, proving that the PAM has successfully adsorbed onto the unbleached pulp fibre surface. It can be noted that the isoelectric point is  $\sim 6.3$ , which is

consistent with previous reported value [19]. Based on these results, pH 8.5 is selected to carry out the deposition of  $\text{CoFe}_2\text{O}_4$  nanocrystals onto the pulp fibres treated with PAM in which both nanocrystals and fibres possess opposite charge.

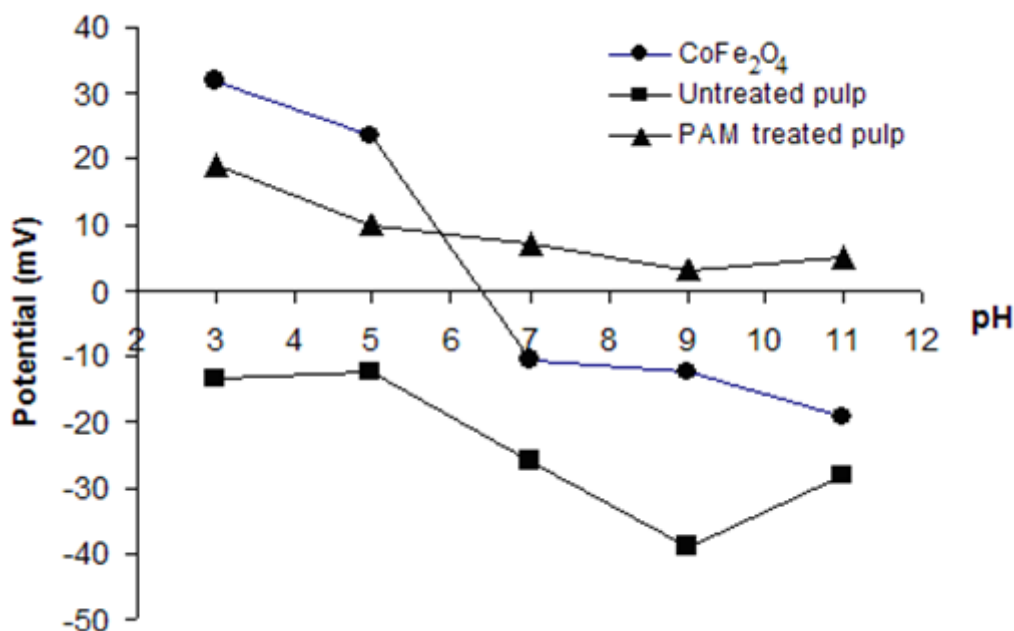


Figure 2: Surface charge of unbleached kenaf pulp fibres (untreated and PAM-treated) and  $\text{CoFe}_2\text{O}_4$  nanocrystals as a function of pH at 25 °C

### 3.3 Deposition of $\text{CoFe}_2\text{O}_4$ Nanocrystals onto Pam-Treated Kenaf Fibre

Figure 3 shows the degree of deposition of  $\text{CoFe}_2\text{O}_4$  nanocrystals onto the pulp fibres at different concentrations of  $\text{CoFe}_2\text{O}_4$  nanocrystals. It can be seen that the amount of  $\text{CoFe}_2\text{O}_4$  nanocrystals deposited onto pulp fibre increases with increasing concentration of nanocrystals. The result from dissolved  $\text{CoFe}_2\text{O}_4$  nanocrystals after deposition fluctuates after the addition of 40 wt%  $\text{CoFe}_2\text{O}_4$  nanocrystals, suggesting the formation of  $\text{CoFe}_2\text{O}_4$  nanocrystals monolayer on the fibre surface. The monolayer capacity was found to be ~115 mg/g with addition of 40 wt%  $\text{CoFe}_2\text{O}_4$  nanocrystals, which is consistent with previous studies reported on the deposition of titanium dioxide [11] and calcium carbonate [9] onto pulp fibres. Fluctuation occurred at deposition concentration of higher than 40 wt% may be due to no more available positive sites on the PAM-treated fibre surface for further deposition



after approaching monolayer coverage. Meanwhile, van der Waals and magnetic dipole-dipole interactions may become dominant for further  $\text{CoFe}_2\text{O}_4$  nanocrystals deposition. These weak interactions between  $\text{CoFe}_2\text{O}_4$  nanocrystals and pulp fibre will result in readily detachment of nanocrystals from the fibre surface.

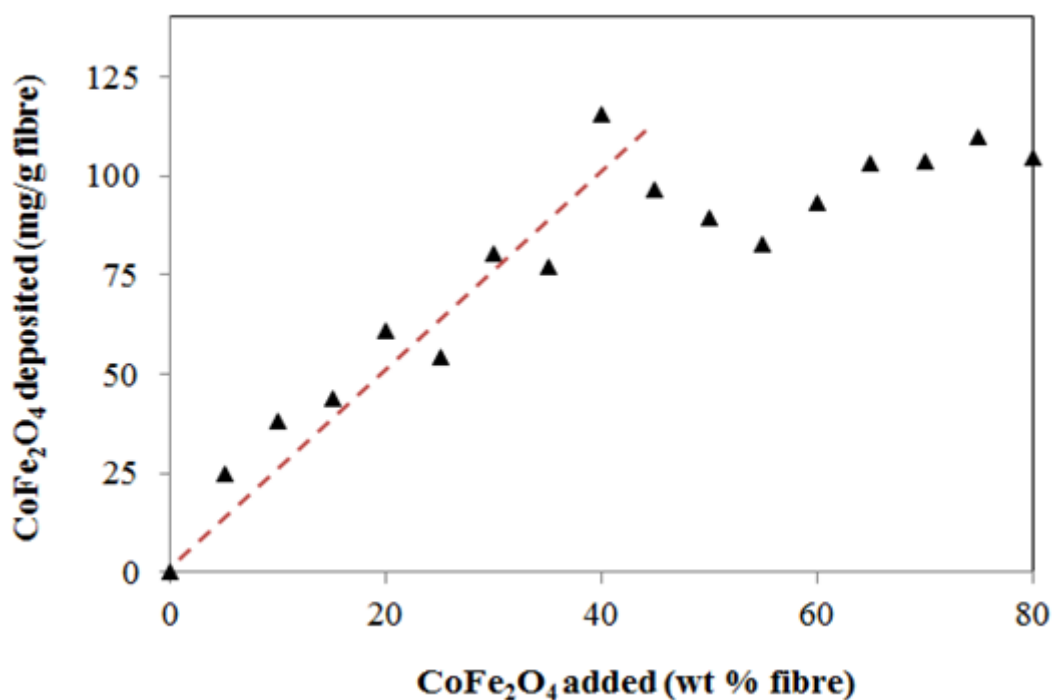


Figure 3: Plots of  $\text{CoFe}_2\text{O}_4$  deposited onto unbleached pulp fibre against the concentration of  $\text{CoFe}_2\text{O}_4$  added (5-100 wt%)

SEM images of the magnetic fibre produced by adding different amount of  $\text{CoFe}_2\text{O}_4$  nanocrystals are shown in Figure 4. This figure reveals the clean and smooth surface of the unbleached kenaf fibres before the deposition process. It can be clearly seen that the  $\text{CoFe}_2\text{O}_4$  nanocrystals have evenly distributed onto the fibre surface with addition of 25 wt% of  $\text{CoFe}_2\text{O}_4$  nanocrystals, as shown in Figure 4 (b). This suggests that the PAM has uniformly attached onto the fibre surface, which will subsequently serve as positive sites for the deposition of  $\text{CoFe}_2\text{O}_4$  nanocrystals.

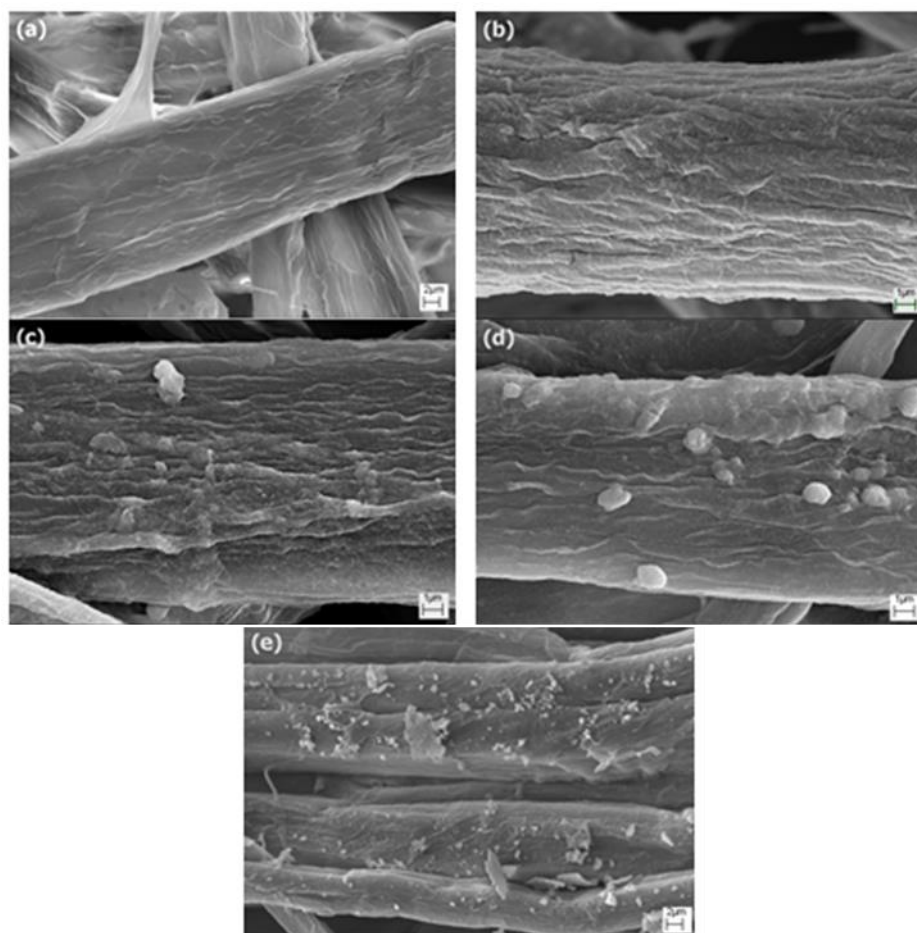


Figure 4: SEM micrographs: (a) control unbleached kenaf fibre; magnetic kenaf fibre produced with addition of (b) 25 wt%, (c) 50 wt%, (d) 75 wt% and (e) 100 wt% of  $\text{CoFe}_2\text{O}_4$  nanocrystals

Figure 4(c) shows the presence of  $\text{CoFe}_2\text{O}_4$  aggregates on the surface of the fibres at the addition of 50 wt% of  $\text{CoFe}_2\text{O}_4$  nanocrystals and the number of the aggregates increases with increasing  $\text{CoFe}_2\text{O}_4$  nanocrystals to 75 wt% (Figure 4 (d)). This may be due to the excess nanocrystals added after the monolayer deposition and no more positive sites is available for further deposition via electrostatic binding. The formation of the aggregates can be attributed to the large surface area to volume ratio of the nanocrystals, leading to the formation of van de Waals and magnetic dipole-dipole interactions between the  $\text{CoFe}_2\text{O}_4$  nanocrystals. It should be noted from Figure 4(e) that the  $\text{CoFe}_2\text{O}_4$  nanocrystals layer deposited on the fibre surface starts to peel off when the addition of  $\text{CoFe}_2\text{O}_4$  nanocrystals

reaches 100 wt%. This can be due to over deposition of CoFe<sub>2</sub>O<sub>4</sub> nanocrystals (including the aggregates) onto the fibre surface, which has resulted in failure of the electrostatic bonding between the first layer of the CoFe<sub>2</sub>O<sub>4</sub> nanocrystals and the fibres. Therefore, from these SEM images, it can conclude that the amount of CoFe<sub>2</sub>O<sub>4</sub> nanocrystals to form monolayer onto the fibre surface is ~50 wt%, which is consistent with the deposition results shown in Figure 3.

### 3.4 Layer-by-Layer Deposition of CoFe<sub>2</sub>O<sub>4</sub> Nanocrystals on Fibres

From the monolayer deposition study above, we found that 40 wt% of CoFe<sub>2</sub>O<sub>4</sub> nanocrystals solution is the ideal concentration for monolayer deposition, hence, this concentration is chosen for LbL deposition process. Figure 5 shows the SEM micrographs of the fibres before and after LbL deposition. It clearly shows that the deposited layers are thicker with increasing deposition layers. For comparison purposes, a sample of magnetic fibres was also produced using *in situ* synthesis method, in which the amount of CoFe<sub>2</sub>O<sub>4</sub> nanocrystals is approximately 200 wt%. PAM was also added into the pulp suspension during the *in situ* synthesis process. The aggregations formed on the fibres of 200 wt% (*in situ* synthesis) and 5-layers of CoFe<sub>2</sub>O<sub>4</sub> nanocrystals (LbL) are quite similar as can be seen in Figure 5(d) and 5(e).

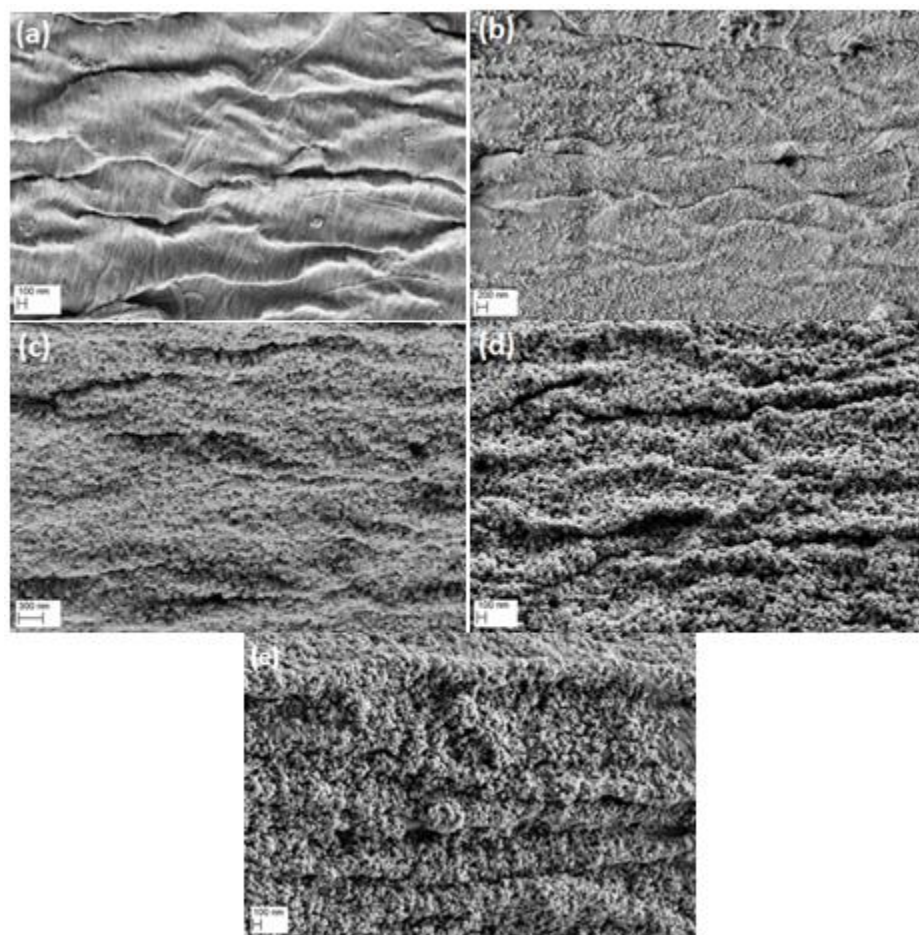


Figure 5: (a) Control unbleached kenaf fibre; magnetic kenaf fibre produced with (b) 1 layer, (c) 3 layers, (d) 5 layers of  $\text{CoFe}_2\text{O}_4$  nanocrystals, and (e) 200 wt% deposited fibres

### 3.5 Detachment of $\text{CoFe}_2\text{O}_4$ Nanocrystals of the Magnetic Paper after Papermaking

Table 1 presents the images of the surface of the magnetic fibres before and after the papermaking process. These images reveal the retention strength of the  $\text{CoFe}_2\text{O}_4$  nanocrystals on the fibre surface when exposed to turbulence created during the papermaking process. As can be seen from the magnetic fibres produced using LBL method, the nanocrystals deposited on the fibre surface are well retained after the papermaking process. However, the detachment was severe for the *in situ* synthesized magnetic fibres, which can be obviously seen that most of the nanocrystals were removed from the fibres surface after the papermaking process. This can be due to weak interaction forces of the upper deposited layer, whereas LbL deposited  $\text{CoFe}_2\text{O}_4$  nanocrystals are held together by electrostatic forces.

Figure 6 shows the degree of loading and saturation magnetization of the magnetic paper samples produced by LbL deposition and also *in situ* synthesis. In general, the degree of loading and saturation magnetization of the magnetic paper increases linearly with the number of LbL deposition layers. Therefore the magnetic properties of the magnetic paper can be fine-tuned by varying the number of LbL deposition layers. In addition, as compared to the magnetic paper produced by *in situ* synthesis, although the amount  $\text{CoFe}_2\text{O}_4$  nanocrystals was approximately the same, but the loading degree of the magnetic paper produced with 5-layers of LbL deposition was much higher. This was due to the high retention strength of the LbL layers of  $\text{CoFe}_2\text{O}_4$  nanocrystals which prevents detachment during the papermaking process.

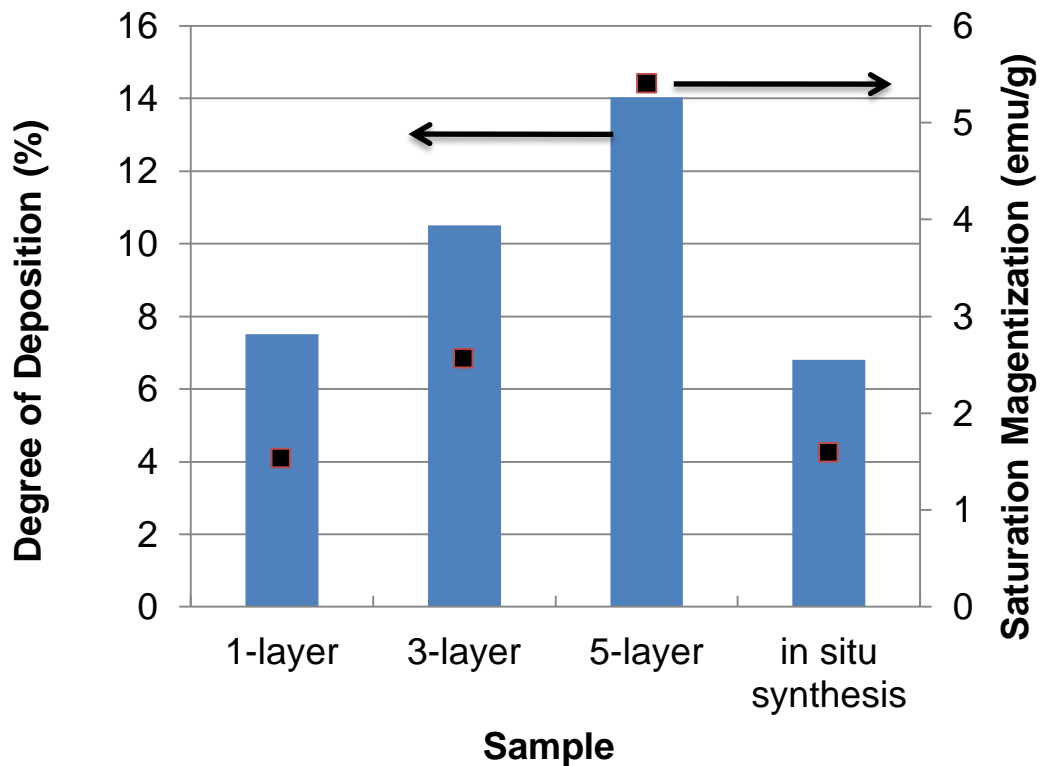


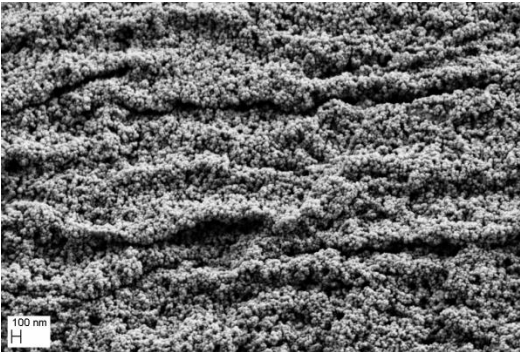
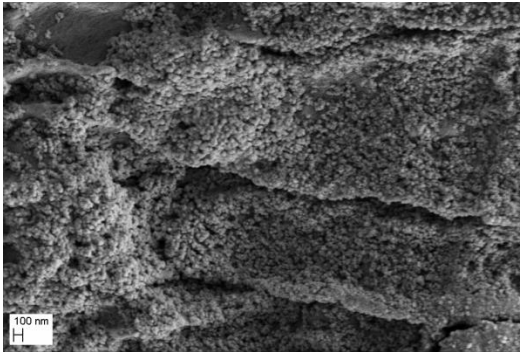

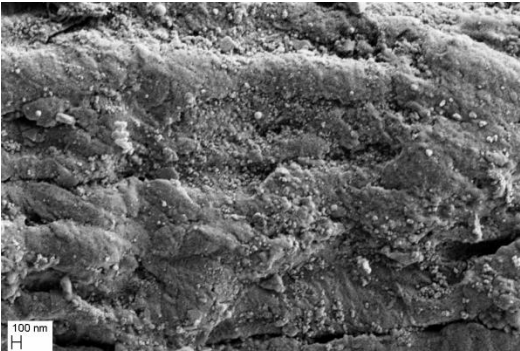


Figure 6: Degree of magnetic loading (wt%) and saturation magnetization (emu/g) of magnetic papers

Table 1: Surface morphology of magnetic fibres produced: before and after papermaking process

Sample	Before Papermaking	After Papermaking
LbL - 3 layers		
LbL - 5 layers		
<i>In situ</i> Synthesis		

### 3.6 Physical Properties of the Magnetic Papers Produced From Magnetic Pulp Fibres

Figure 7 shows the tensile index of the control kenaf paper and magnetic papers. The addition of PAM has slightly increased the tensile strength of the control kenaf paper. The tensile strength of the produced magnetic paper was decreased with the increase of the number of deposition layers. Magnetic paper made from magnetic fibres of 5-layers of  $\text{CoFe}_2\text{O}_4$  nanocrystals decreased in strength as much as 50.0 % from 44.27 Nm/g of the

control kenaf paper sample to 23.59 Nm/g due to increasing thickness layer which interfered the fibre-fibre bonding. The magnetic paper produced by *in situ* synthesis method possessed higher tensile strength as compared to the LbL samples, which can be attributed to the lower degree of magnetic loading.

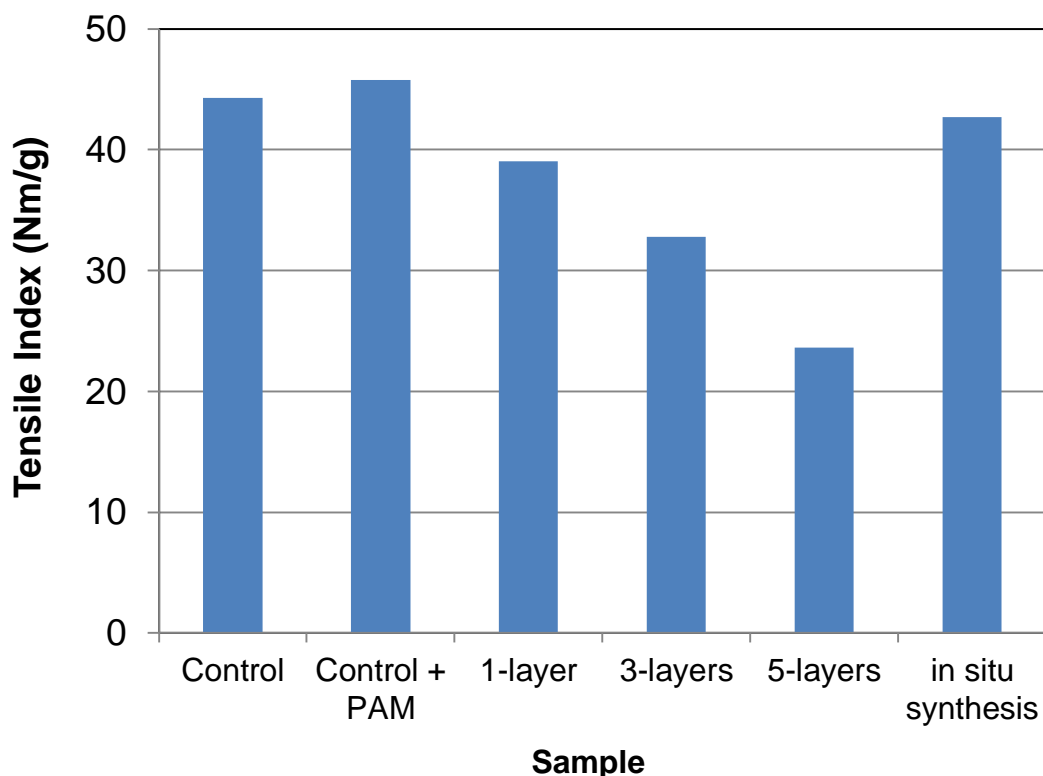


Figure 7: Tensile index (Nm/g) of paper from fibres and magnetic fibres

#### 4.0 CONCLUSIONS

Magnetic fibres are successfully produced using LbL deposition method. Prior to the deposition experiment, the negative charge of the fibre has been changed to positive using PAM to allow the deposition of the negative charge  $\text{CoFe}_2\text{O}_4$  nanocrystals onto the fibre surface via electrostatic interaction. The amount of  $\text{CoFe}_2\text{O}_4$  nanocrystals deposited onto the fibre increases linearly to 115 mg/g of fibre with increasing addition of  $\text{CoFe}_2\text{O}_4$  nanocrystals to 40 wt%. A 5-layer magnetic paper showed an increase of 240 % in magnetic strength compare to 200 wt% deposited magnetic paper but with a decrease of 50 % in tensile index



compared to control sample.  $M_s$  of 5.41 emu/g is obtained for a 5-layer magnetic paper as compared to  $\text{CoFe}_2\text{O}_4$  nanocrystals which is 36.4 emu/g.

## ACKNOWLEDGEMENTS

The authors acknowledge the financial support given by Universiti Kebangsaan Malaysia for the financial support via the research project grants UKM-GGPM-NBT-085-2010, UKM-OUP-FST-2012 and UKM-FST-07-FRGS0233-2010.

## REFERENCES

1. S. Zakaria, B. H. Ong, S. Ahmad, M. Abdullah. Preparation of lumen-loaded kenaf pulp with magnetite. *Materials Chemistry and Physics* 2005, (89):216.
2. S. Zakaria, B.H. Ong, T.G.M. van de Ven. Lumen loading magnetic paper I: flocculation. *Colloid and Surfaces A: -Physicochemical and Engineering Aspects* 2004, (251):1.
3. C.H. Chia, S. Zakaria, S. Ahmad, M. Abdullah, S. Mohd Jani. Preparation of magnetic paper from kenaf: lumen loading and in situ synthesis method. *American Journal of Applied Sciences* 2006, (3):1750.
4. A.C. Small, J.H. Johnson. Novel hybrid materials of magnetic nanoparticles and Cellulose Fibres. *Journal of Colloid and Interface Science* 2009, (331):122.
5. C.H. Chia, S. Zakaria, K.L. Nguyen, M. Abdullah. Utilisation of unbleached kenaf Fibres for the preparation of magnetic paper. *Industrial Crops and Products* 2008, (28):333
6. D. Zhao, X. Wu, H. Guan, E. Han. Study on Supercritical hydrothermal synthesis of  $\text{CoFe}_2\text{O}_4$  nanoparticles. *Journal of Supercritical Fluids* 2007, (42):226.
7. M.M. de Villiers, D.P. Otto, S.J. Strydom, Y.M. Lvov. Introduction to nanocoatings produced by layer-by-layer (LbL) self-assembly. *Advanced Drug Delivery Reviews* 2001, (63):701.
8. Z. Lu, S. Eadula, Z. Zheng, K. Xu, G. Grozdits, Y. Lvov. Layer-by-layer nanoparticle coatings on lignocellulose wood microfibrils. *Colloid and Surfaces A: -Physicochemical and Engineering Aspects* 2007, (292):56.
9. S.R. Middleton, A.M. Scallan. A kinetic-model for the adsorption of fillers by pulp fibres. *Journal of Pulp and Paper Science* 1991, (17):127.
10. R.A. Gill. Interactions between polymers and precipitated calcium carbonate filler. *Nordic Pulp and Paper Research Journal* 1993, (8):167.
11. S.R. Middleton, J. Desmeules, A. M. Scallan. Lumen loading with calcium carbonate fillers. *Journal of Pulp and Paper Science* 2003, (29):241.
12. M. Kamiti, T.G.M. van de Ven. Kinetics of deposition of calcium carbonate particles onto pulp fibres. *Journal of Pulp and Paper Science* 1994, (20):199.
13. T.G.M. van de Ven. Particle deposition on pulp fibres. *Nordic Pulp and Paper Research Journal* 1993, (8):130.
14. S.R. Middleton, A.M. Scallan. Lumen-loaded paper pulp: mechanism of filler-to-fibre bonding. *Colloids and Surfaces* 1985, (6):309.
15. B. Alinec, R. Lebreton, S. St-Amour. Using cationic starch in filled papers. *Tappi Journal* 1990, (73):191.



16. F. Aloulou, S. Boufi, D. Beneventi. Adsorption of organic compounds onto polyelectrolyte immobilized-surfactant aggregates on cellulosic fibres. *Journal of Colloid and Interface Science* 2004, (280):350.
17. L. Chitu, M. Jergel, E. Majkova, S. Luby, I. Capek, A. Satka, J. Ivan, J. Kovac, M. Timko. Structure and magnetic properties of  $\text{CoFe}_2\text{O}_4$  and  $\text{Fe}_3\text{O}_4$  nanoparticles. *Materials Engineering C* 2007, (27):1415.
18. N.K. Bhardwaj, T.D. Duong, K.L. Nguyen. Pulp charge determination by different methods: effect of beating/refining. *Colloid and Surfaces A: Physicochemical and Engineering Aspects* 2004, (236):39.
19. J.d. Vicente, J.D.G. Durán, A.V. Delgado. Electrokinetic and viscoelastic properties Of magnetorheological suspensions of cobalt ferrite. *Colloid and Surfaces A: Physicochemical and Engineering Aspects* 2001, (195):181.